Latin American Journal of Solids and Structures
www.lajss.org

A Comparison between different techniques for optimum design of steel frames subjected to blast

Abstract
According to the conditions of today's world, design of resistant structures against blast loading is an important subject that requires special attention. Thus, given the benefits of optimization in engineering, development and assessment of optimization methods for optimum design of structures against blast is of great importance. In this research, the optimum design of steel frame structures against blast loading is investigated. For this purpose first an optimization methodology is proposed. In the proposed method the structural analysis is performed using nonlinear explicit finite element analysis. Based on the proposed method a framework is developed and three numerical examples are investigated using different numerical optimization techniques. Results of this study show that by using nonlinear explicit FE analysis as the structural analysis method and NLPQLP optimization technique as the optimization method, the current optimization problem can be performed effectively, because the procedure is relatively accurate and computationally inexpensive.

Keywords
Optimization; blast; nonlinear analysis; steel frames; SQP; NLPQLP; PSO; MIGA

Nima Khaledy[a]
Alireza Habibi[b*]
Parham Memarzadeh[a]

[a] Department of Civil Engineering, Najafabad branch, Islamic Azad University, Najafabad, Iran. E-mail: khaledy83@gmail.com, p-memar@iaun.ac.ir

[b] Department of Civil Engineering, Shahed University, Tehran, Iran. E-mail: ar.habibi@shahed.ac.ir

*Corresponding Author

http://dx.doi.org/10.1590/1679-78254952

Received: March 04, 2018
In Revised Form: June 18, 2018
Accepted: June 29, 2018
Available Online: July 10, 2018

1. Introduction

In today's world, terrorist attacks and wars are phenomena which threaten human security all over the world. Meanwhile, structures play an important role in either increasing or decreasing damages or losses. Also as it's true for other types of loads, if a structure is to be designed to have an appropriate performance against potential events and their subsequent loadings, it will bring psychological comfort for residents and the whole society even though they never occur. Thus, it is very important to conduct more studies on the behavior of structures against blast and the resistant design of structures against this type of loading, particularly under current conditions and events in the world.

Preliminary researches on blast loading, behavior and resistant design of structures against blast date back to the years of World War II (Taylor 1940, 1941a, 1941b). But most studies in this field have been conducted in about past 15 years. Some of the most important researches in recent years carried out on steel structures are as follows:

Hadianfard et al. (2012) studied the effect of steel columns cross sectional properties on their behaviors when subjected to blast. Using ANSYS software, they analyzed some steel columns with different shapes of cross-section and different boundary conditions, subjected to blast loading. They concluded that shape and elastic-plastic properties of sections and also boundary conditions of columns play important roles on the response of steel columns subjected to blast.

Nassr et al. (2012) modeled steel beam and beam-columns against blast load using single and multi-degree of freedom models. First, they conducted an experimental study to evaluate responses of some wide flange beams subjected to blast. Then, they compared the results of the SDOF and MDOF models with the experimental tests. Based on the results, it was shown that both proposed single and multi-degree of freedom models could predict the history of responses with a good accuracy. Also, they concluded that the use of a constant strain rate to calculate Dynamic Increase Factor (DIF) would lead to a conservative design.

Using passive unidirectional dampers, Saeed Monir (2013) conducted a research on the resistant steel structures against blast. He presented a new uni-directional passive damper which shows different performance

against compression and tension. He concluded that using this type of damper in a ductile frame, a resistant structure would be obtained which it could absorb most of the blast energy.

Nassr et al. (2013) evaluated the resistance and stability of steel beam-columns subjected to blast loading. They used a one-degree of freedom model for studying the effects of axial load on the strength and stability of columns subjected to blast. The model was validated by comparing the results with experimental results and also finite element analysis. Comparing the results of the one-degree of freedom model and results from UFC 3-340-02 code, showed that regardless of axial load to the Euler critical load ratio, the UFC method overestimates the column's capacity for ductility coefficients greater than one.

Coffield and Adeli (2014) examined the performance of earthquake-resistant bracing systems against blast. They studied three systems including Moments Resistant Frame (MRF), a Centrally Braced Frame (CBF) and an Eccentrically Bracing Frame (EBF), designed for earthquake. The results showed that the CBF system had a better resistance level in the blast scenarios considered in the study.

Elsanadedy et al. (2014) studied the potential of progressive collapse in steel structures subjected to blast attacks. They analyzed a conventional multi-story steel frame against blast to evaluate its vulnerability in accidental or terroristic blast scenarios. Based on the results of finite element analysis, they proposed strategies for reducing and controlling potential progressive collapse in steel structures.

Habibi and Khaledy (2015) proposed an analytical method for analyzing beam-columns against lateral blast load. Assuming elastic behavior for beam-column, the governing fourth-order partial differential equation was formulated, and then an analytical method for solving this differential equation was proposed. By studying a numerical example, they concluded that the influence of axial force on lateral displacement of the beam-columns is very significant and practically this effect should not be neglected. Also, it was concluded that for different values of axial force, the maximum lateral deformation does not occur at a specified time and the time is a function of the applied axial force.

On the other hand, optimum design of structures given numerous advantages such as cost and time savings is of great importance in structural engineering. Due to advances in the fields of computers and processors, optimization science has undergone a great progress. It is always updated along with new situations and needs of the day. Some of the important researches have carried out on the optimization of steel structures in recent years are as follows:

Degertekin (2012) studied the optimum design of geometrically nonlinear steel frames using artificial bee colony algorithm (ABC). Structural weight minimization was the objective of the research while strength, displacement and size constraints were taken into account. The optimization was performed considering the geometrical nonlinearity. Three numerical examples where studied in the research using the ABC algorithm. He concluded the ABC algorithm could find better results comparing to the other meta-heuristic algorithms.

Kaveh et al. (2010) studied the optimum seismic performance based design of steel frames using Ant Colony algorithm. To get the response of the structure at various performance levels, the nonlinear pushover analysis was performed using a computer. The structural weight was chosen as the objective function, and story drifts were selected as the constraints. In two numerical examples, they showed that the used method is superior to the traditional Genetic Algorithm.

Based on the history of nonlinear responses, Gong et al. (2012) presented a method for optimum design of steel frames under seismic loads. Minimization of weight, minimization of input earthquake energy and maximization of energy absorption, were considered as the three objective functions. Also, story drift and plastic hinge rotation in members were considered as design constraints. A three story building was studied as a numerical example. They concluded that the proposed method is an efficient method for designing steel frames under seismic loadings.

Habibi and Rostami (2013) developed an optimization method for designing steel frames based on Consistent Approximation (CONAP) method. Structural weight was considered as the objective function, and design constraints were considered based on AISC and Iranian steel structures design Code. Having studied multiple numerical examples, they concluded that the proposed method could easily be used to achieve economic and reliable designs. Also, it was shown that the proposed algorithm would converge in a limited number of iterations.

Kaveh and Nasrollahi (2014) conducted a research on optimum performance based on seismic design of steel frames using charged system search (CSS) algorithm. The analysis of structure was performed using pushover approach assuming semi-rigid connections. Based on the results, they concluded that the proposed method would significantly reduce the weight of the structure compared to a traditional design.

Kaveh et al. (2015) studied the optimum design of steel frames considering construction cost and seismic damage. They used Park-Ang damage index for the seismic damage and constraints were considered based on

FEMA-350 seismic design specifications. They adapted the non-dominated sorting genetic algorithm (NSGA II) as the multi-objective optimization technique. They concluded that the proposed framework is effective for achieving convenient pareto front of possible optimal solutions.

Artar (2016) studied the optimum design of braced steel frames using teaching learning based optimization (TLBO). The optimization problems were performed based on AISC-ASD design specifications. Structural weight minimization was the design objective. Design constraints were considered as stress, geometrical size, displacement and inter-story drifts. By studying two numerical examples they concluded that the TLBO is a robust and applicable method for optimum design of multi-element structures.

Gholizadeh et al. (2017) studied optimum design of steel frames using moth-flame optimization (MFO) and enhanced moth-flame optimization (EMFO) algorithms. By solving some benchmark problems using MFO and EMFO, and comparing the results with results of the other meta-heuristic methods, they concluded that the proposed EMFO method had better optimal results while it needed less computational efforts.

In the field of optimum design of structures against blast, researches are just limited to few researches on non-building and non-framed structures (Taha et al. 2009; Sun 2011, Salimi et al. 2012; Qi et al. 2013; Xia et al. 2015). Thus, there is a gap on the field to be filled by more researches on this important subject and related topics. The main purpose of the present study is to compare the efficiency of the three optimization techniques for optimum design of steel moment frames under blast, based on a proposed procedure.

2. Blast Loading

To design structures against blast, it is required to be specified the characteristics of blast loading. Blast load is a time-history loading which occurs in a very short period. Generally, its time-history diagram is as shown in Fig. 1.

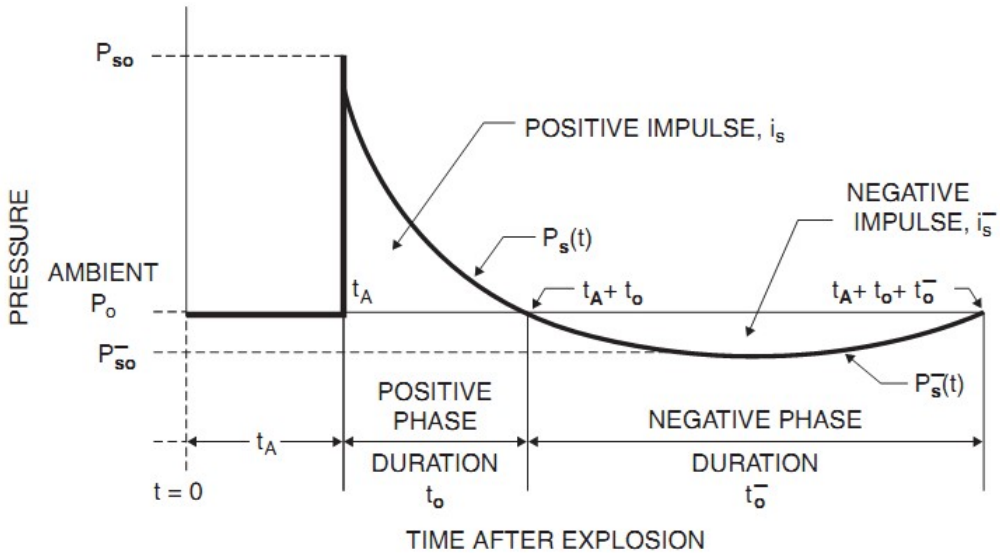

Fig.1*. General time-history diagram for blast loading (UFC 3-340-02, 2008)*

When an explosion occurs on the earth surface or in front of a structure where blast waves can be reflected, this reflection amplifies the blast loading, and in this case, the effective blast pressure would be P_r which is shown in Fig.2.

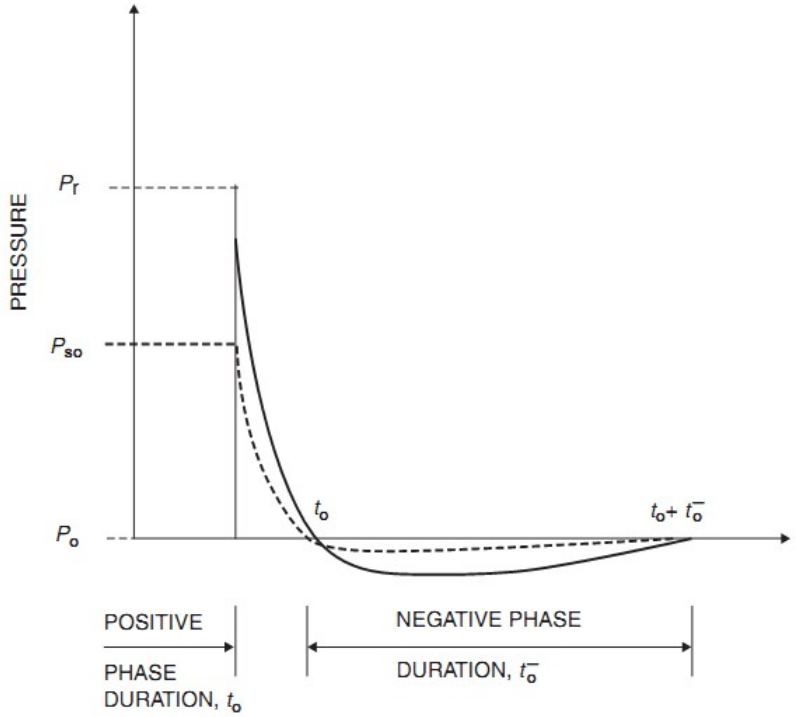

Fig. 2. *Blast load time-history with reflection of waves (UFC 3-340-02, 2008)*

Explosions which occur on the surface of the earth are called Surface bursts (blasts), and explosions which occur in the air are called Air bursts (blasts). The most important parameters associated with blast loading, include maximum effective pressure (P_r or P_o), impulse (the area under time-pressure diagram), and the duration of the positive phase, respectively. As shown in Figs 1 and 2, the time-history diagram of blast loading has two phases, a positive phase (pressure) and a negative (suction) one. In conventional explosions, the negative phase is usually neglected in calculations due to its small magnitude. Duration of blast loading is generally in the range of milliseconds to a few hundredth of a second. It should also be noted that all of the main parameters related to the blast loading are functions of type and mass of the explosive, the distance between explosion source and the target (structure), and the type of the blast (Surface or Air). Calculation of these parameters can be made by some empirical equations or graphs that are presented in references such as UFC 3-340-02 (2008), Blast Effects on Buildings (Cormie et al. 2009) and AISC 59-11 (2011). An example of these graphs related to the surface blasts is shown in Fig. 3.

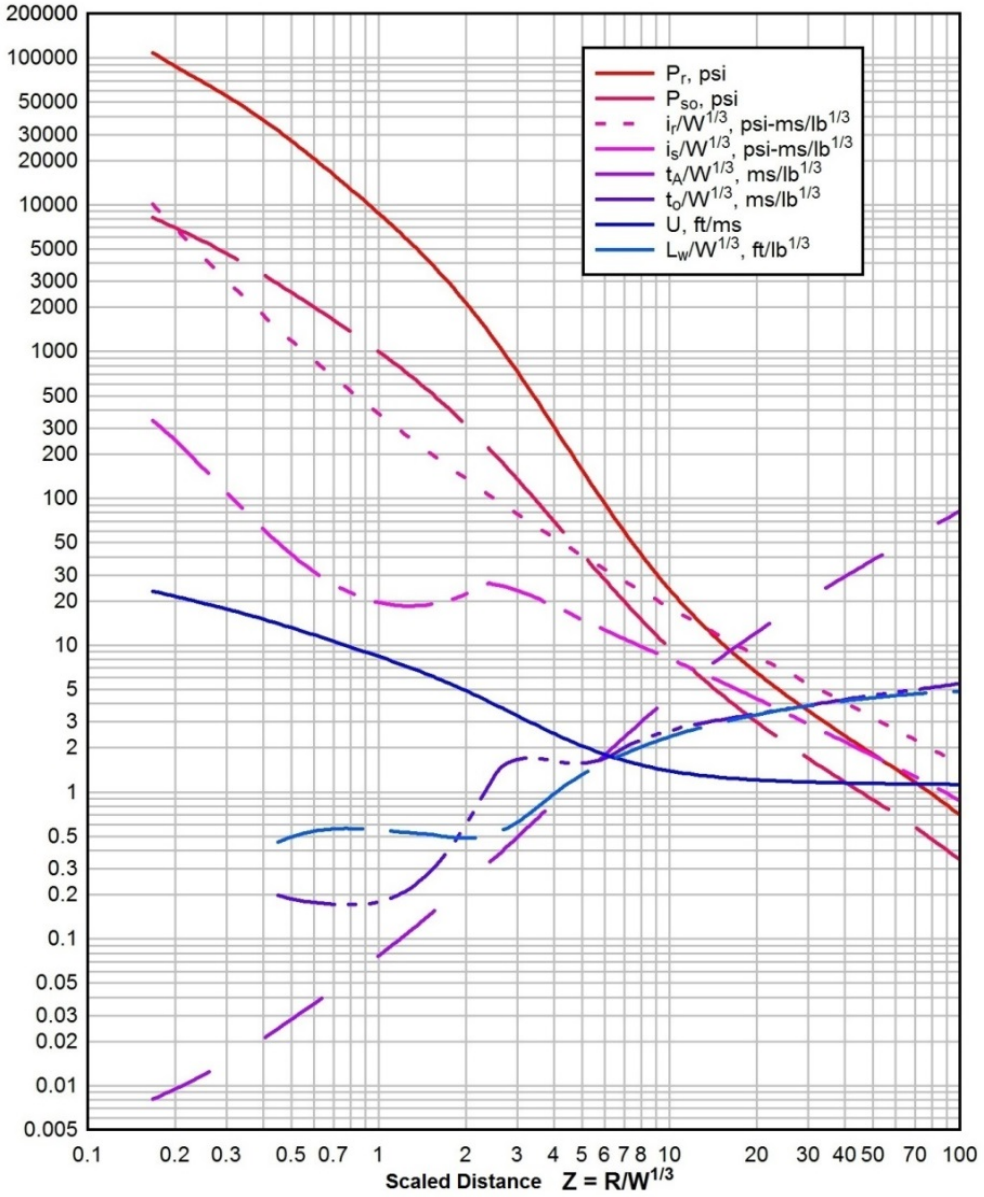

Fig. 3*. A diagram for calculating blast loading parameters in surface blasts (UFC 3-340-02, 2008)*

In this graph Z is the scaled distance of blast:

$$\boldsymbol{Z = \frac{R}{W^{1/3}}} \tag{1}$$

Where R is the distance between blast source and structure, called standoff distance and W is the mass of equivalent TNT of explosive. All of the graphs and equations for calculating blast-related parameters are set based on TNT. For other types of explosives, the mass must be multiplied by some coefficients in order to be able to use the graphs. For some explosive types, these coefficients are shown in Table 1.

Table 1 Equivalent TNT mass for some explosives (Cormie et al. 2009)

Explosive Material	TNT equivalent factor
Nitroglycerin	1.481
C4	1.19 to 1.37
Semtex	1.256
RDX	1.185
TNT	1
ANFO	0.87

In blast events, the effective pressure decreases as a nonlinear function by moving away from the source of the explosion, so that the local effects should be considered in near-range explosions. Based on ASCE 59-11 (2011) if the scaled distance Z be greater than $\mathbf{3}\ \boldsymbol{ft/lb^{1/3}}$ ($\mathbf{1.2}\ \boldsymbol{m/kg^{1/3}}$) the explosion is classified as far-range, and the loading can be considered as a uniform distributed time-history load acting on the structure. In the current study, blast events are assumed to be in the far range.

The quantity and blast characteristics a given structure is designed for, depends on various factors such as the history of terrorist attacks, the importance of the building, ease of access to the building or terroristic target, the number of occupants of the building, distance from the structure and ease of access to the threatening materials (FEMA 452, 2005). Based on these factors, a simplified method is proposed in FEMA 452 for terroristic threats risk assessment. Also, there are some diagrams which can be used to estimate the potential blast capacity of some blast threats. One of these diagrams is shown in Fig. 4. For example, based on this diagram, a sedan car has a capacity of carrying a mass between 100-500 lbs. (45-226 kg) of TNT.

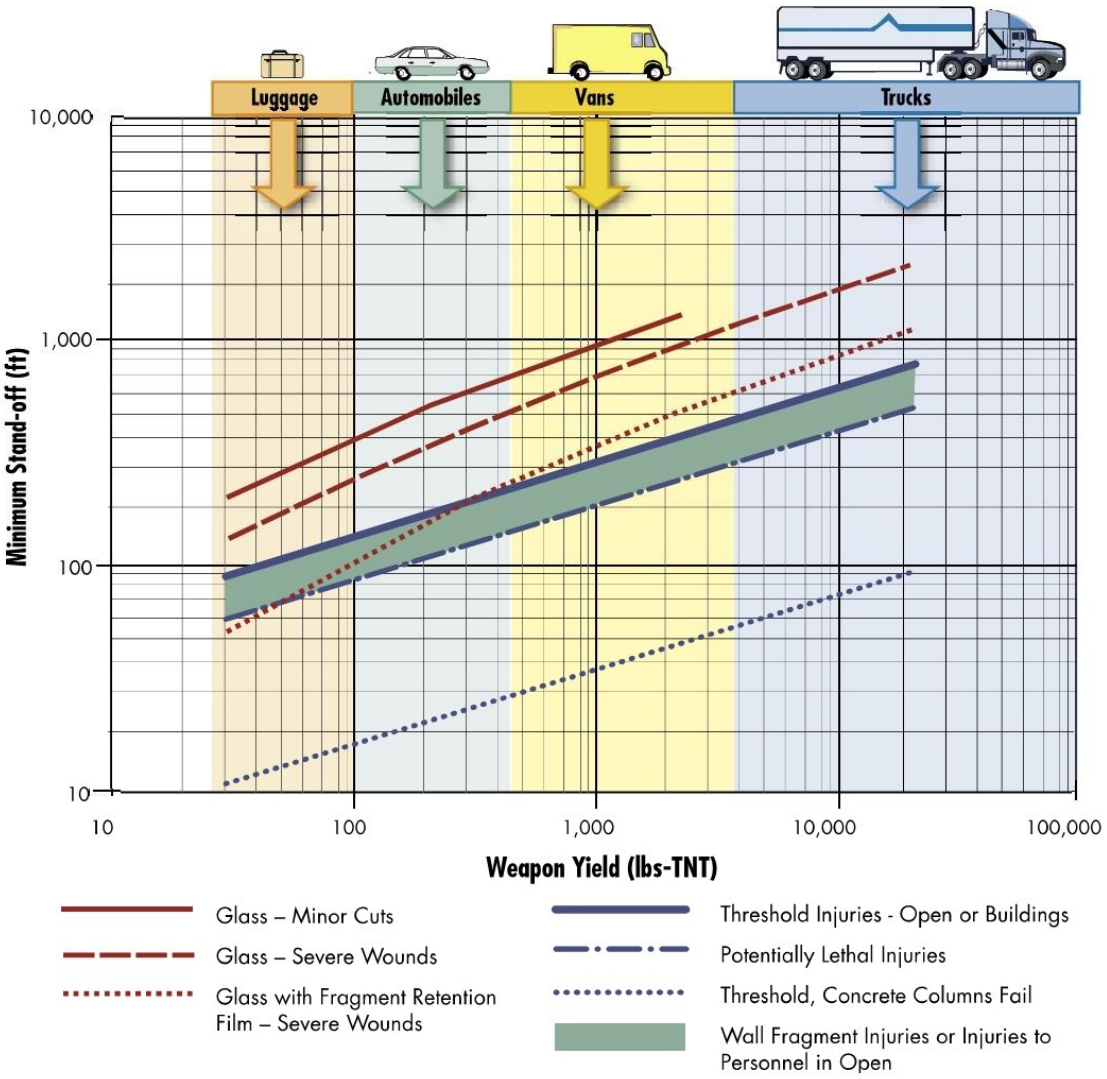

Fig. 4. *Explosive environments- blast range to effect (FEMA 452, 2005)*

3. Nonlinear dynamic analysis

In this research, the structural analysis has been performed by finite element analysis using Abaqus software (Hibbitt et al., 2010). In the finite element analysis, the nonlinear dynamic analysis is performed by direct integration methods. Direct integration methods can be performed by two different procedures: Implicit approach and explicit approach. In the "implicit" approach, it is required that in every step the structural stiffness matrix be inverted and nonlinear equations be solved. Thus, when the degrees of freedom are high, this method will be computationally expensive as it is required to calculate the inverse of the stiffness matrix and solve the nonlinear equations. In the "explicit" approach, velocity and displacement are calculated based on the known values at the beginning of each time step. Therefore, calculating the inverse of the stiffness matrix is not required. In other words, compared to the implicit method, this method requires less computational effort at each time step. However, the "implicit" method is numerically stable, while in "explicit" approach, time steps should be considered small enough to ensure the stability of the method. Thus, in dynamic problems that occur in a short time such as impact and explosion problems, the explicit method is better and requires less computational effort. Because of the mentioned computational advantages, the explicit method is used in this research.

One of the most popular explicit methods is the central difference method. In this method velocity and accelerations are written as follows (De Borst et al., 2012):

$$\dot{u}^{t+\Delta t} = \frac{u^{t+\Delta t} - u^{t-\Delta t}}{2\Delta t} \tag{2}$$

$$\ddot{u}^{t+\Delta t} = \frac{u^{t+\Delta t} - 2u^t + u^{t-\Delta t}}{\Delta t^2} \tag{3}$$

Where $u, \dot{u}$, and $\ddot{u}$ are the displacement, velocity, and acceleration vectors, respectively. Also, Δt is the time step. We can write the equation of motion as follows:

$$M\ddot{u}^{t+\Delta t} = f_{ext}^{t+\Delta t} - f_{int}^{t+\Delta t} \tag{4}$$

Where, M is the global mass matrix, and f_{ext} and f_{int} are the external and internal forces vectors, respectively. By substituting Eq(3) in Eq(4) we have:

$$\frac{1}{\Delta t^2} M u^{t+\Delta t} = f_{ext}^{t+\Delta t} - f_{int}^{t+\Delta t} + \frac{1}{\Delta t^2} M(2u^t - u^{t-\Delta t}) \tag{5}$$

This equation can be solved for displacement in $t + \Delta t$:

$$u^{t+\Delta t} = \Delta t^2 M^{-1}\left(f_{ext}^{t+\Delta t} - f_{int}^{t+\Delta t}\right) + 2u^t - u^{t-\Delta t} \tag{6}$$

Then the displacement increment can be calculated as $\Delta u = u^{t+\Delta t} - u^t$, and the strain increment $\Delta\epsilon$ will be obtained based on the Kinematic relation. Then the stress increment $\Delta\sigma$ can be obtained using the constitutive equations. The stress is updated using the following equation:

$$\sigma^{t+\Delta t} = \sigma^t + \Delta\sigma \tag{7}$$

And the internal forces vector can be derived as follows:

$$f_{int} = \sum_{e=1}^{n_e} Z_e^T \int_{V_e} B_T \sigma dV \tag{8}$$

Where n_e is the number of elements, Z_e is the incidence or location matrix which relates the local and global coordinates of an element, and B is a matrix that relates the strains within an element with the nodal displacements. The above integration can be solved using numerical techniques like Gaussian or Simpson numerical integration techniques. Since in Eq(6) the displacement in $t + \Delta t$ is calculated based on the displacement in t and $t - \Delta t$, thus the displacement values in the two previous steps are required. This makes an initialization problem for t=0. To overcome this issue, the Eq(6) for t=0 is written as follows:

$$u^{-\Delta t} = u^0 - \Delta t\dot{u}^0 + \frac{1}{2}\Delta t^2 M^{-1}\left(f_{ext}^0 - f_{int}^0\right) \tag{9}$$

Where, u^0 and $\dot{u}^0$ are the initial displacement and the initial velocity vectors.

In the present study, we have modeled the frame structure using B21 Timoshenko beam element (Hibbitt et al., 2010). Also, material nonlinearity is considered as bilinear elasto-plastic steel with isotropic hardening. Also, geometrical nonlinearity is considered in the analysis. Elements sizes (mesh size) are chosen by 1/10 of member's length. Also, strain rate effects are considered in the analysis according to UFC 3-340-02 (2008) as shown in Fig.5. To ensure the accuracy of the finite element model, this model has been validated by another study. Nassr (2012) experimentally and analytically studied the response of some beam and beam-columns against blast. Here, two beams and two beam-columns which had been studied by Nassr are modeled. In the modeled samples, each member length is 2413 mm and section profiles are W150X24. The shape and dimensions of W150X24 section profile is shown in Fig 6. Yield stress of the steel material is 470 MPa as reported by Nassr. Since the yield stress is 470 MPa, and there is no specific curve for steel with Fy=470 MPa in Fig 5, thus, the DIF data have been interpolated between the curves for ASTM A36 (Fy=250 MPa) and ASTM A514 (Fy=700 MPa) to be used in FE modeling of the experimental tests. The experimental test setup is shown in Fig 7. Also, a schematic drawing of the location of the charge and the samples is shown in Fig 8. Summary of the modeled tests in the present study is shown in Table 2. Complete details of the experimental tests are described by Nassr (2012).

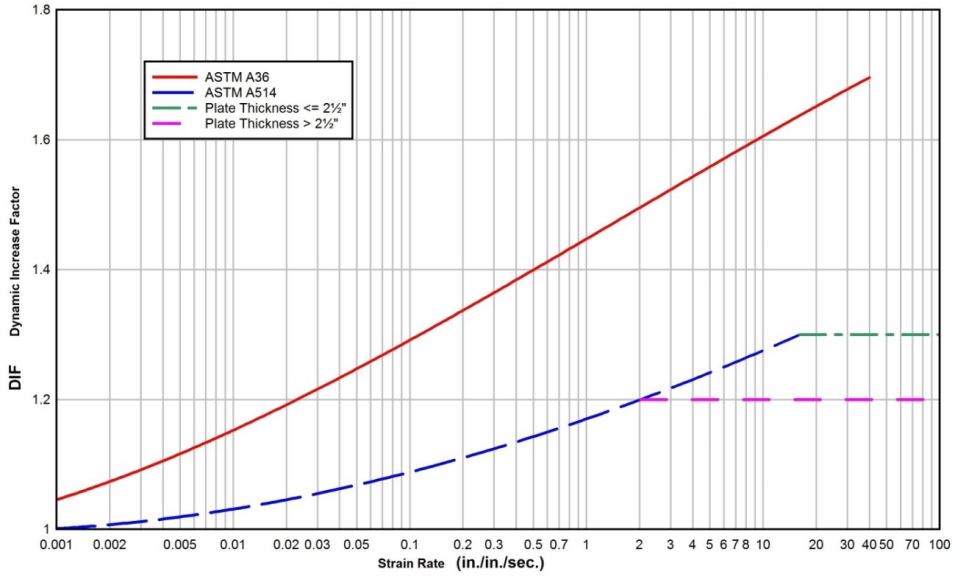

Fig. 5*. Strain Rate Effect (SRE) on Dynamic Increase Factor (DIF) (UFC 3-340-02, 2008)*

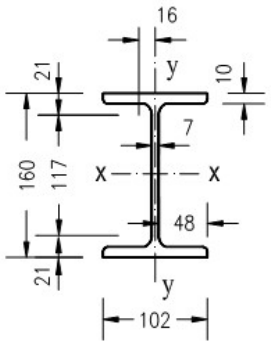

Fig. 6. *Cross-sectional shape and dimensions of the test samples (all dimensions are in mm)*

Fig. 7. *The experimental test setup (Nassr, 2012)*

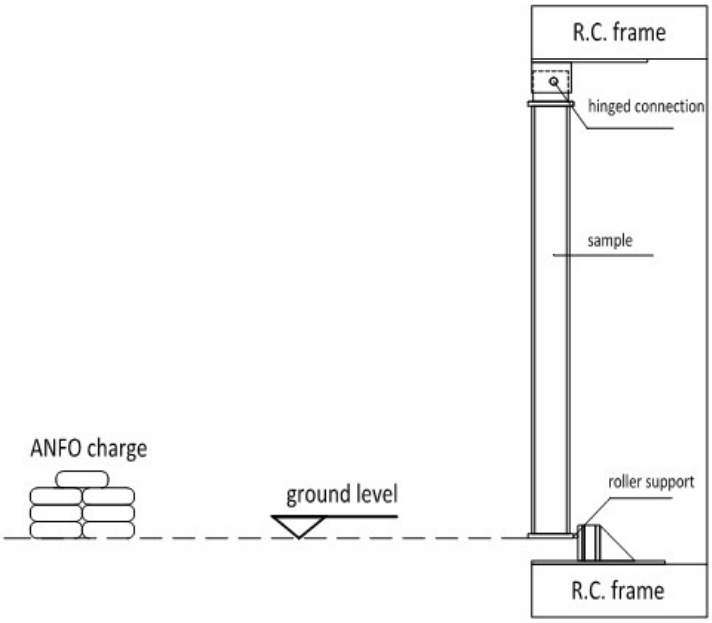

Fig. 8. *Schematic drawing of the charge and the samples location (Nassr, 2012)*

Table 2. *Properties of the experiments selected for FE model validation*

Sample Name	Bending Axis	Axial Load *(kN)*	standoff *(m)*	Charge mass *ANFO (kg)*
B1	*x-x*	0	10.3	50
B2	*x-x*	0	9	150
C1	*y-y*	270	10.3	100
C2	*x-x*	270	9	150

In Figs 9 to 12, history of mid-span deflection of modeled samples in the current study and the results reported by Nassr are compared. As it is obvious, the used finite element model properly predicted the history of mid-span deflection of the members. In Figs 9-12, differences between the maximum mid-span deflection in the current study and the experimental study of Nassr (2012) are 1.4%, 2.8%, 0 and 3.1% respectively. Also in these Figs, it is evident that the history of responses in the current study and the multi-degree of freedom model used by Nassr have a high compatibility with each other. In both studies, beam elements are used. In the current study, each member is divided into 10 elements, and the Timoshenko beam elements are used. Nassr had used Bernoulli beam elements, and each member was divided into 24 elements. It should be noted that in the process of verification it was observed that the sensitivity of responses was high to changes in the maximum blast pressure and the blast duration. Therefore, it seems that the very small differences in graphs, is due to the very small differences in the blast loading in the experimental test and the numerical model. In the current study, the blast load applied to the members by a uniform distributed time-history load, which in the experiments, based on the pressures measured by gauges, the pressure distribution had not been completely uniform over the member's length. In addition, in real conditions, due to shape and type of obstacles in the field, and the effect of reflection of blast waves, the actual diagram of blast loading may not be exactly as the diagrams obtained by the equations and curves presented in manuals and design codes, which probably are derived in some specific and simplified conditions. It should be emphasized that the horizontal axes of the verification diagrams are in millisecond, and therefore differences between the compared graphs are very small.

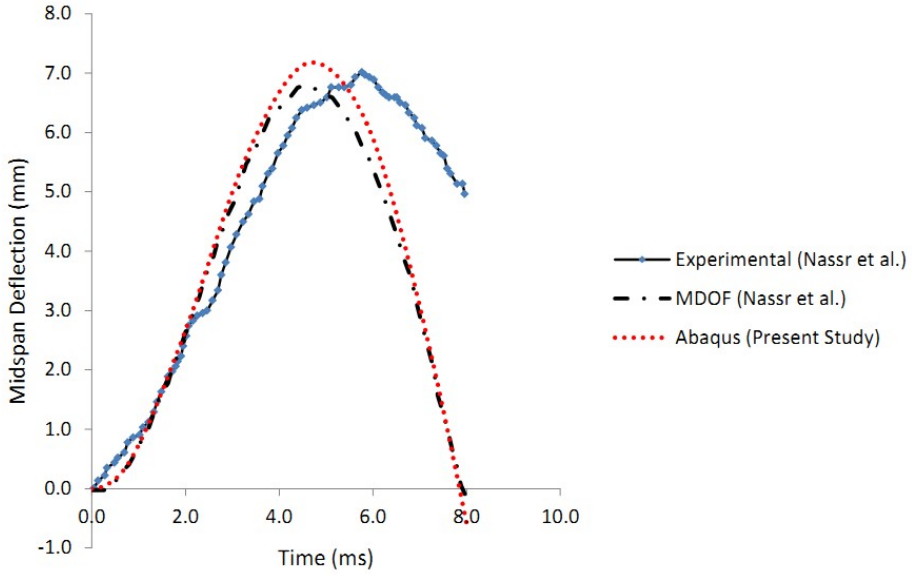

Fig. 9. *Mid-span deflection of B1 beam*

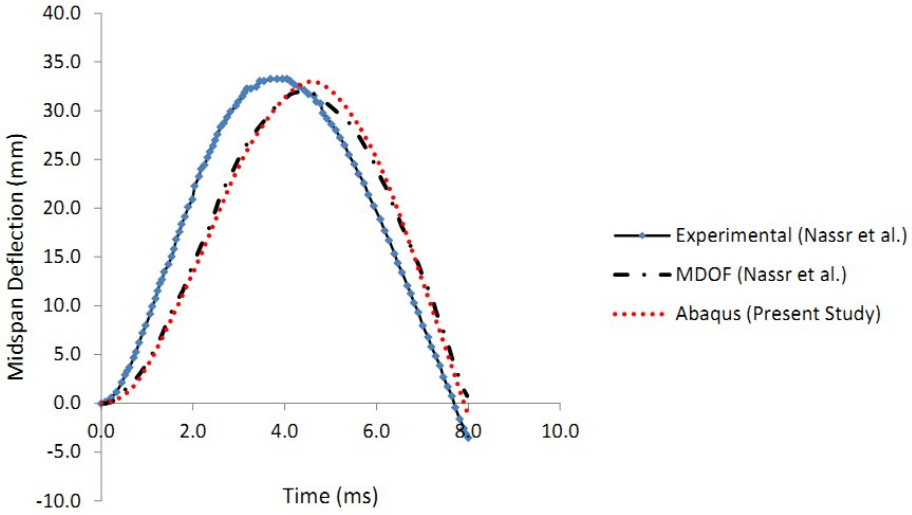

Fig. 10. *Mid-span deflection of B2 beam*

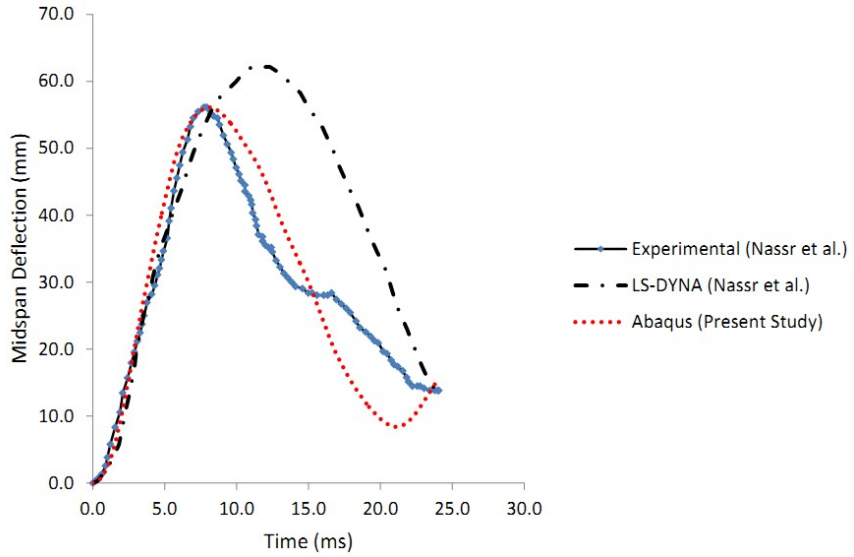

Fig. 11. *Mid-span deflection of C1 column*

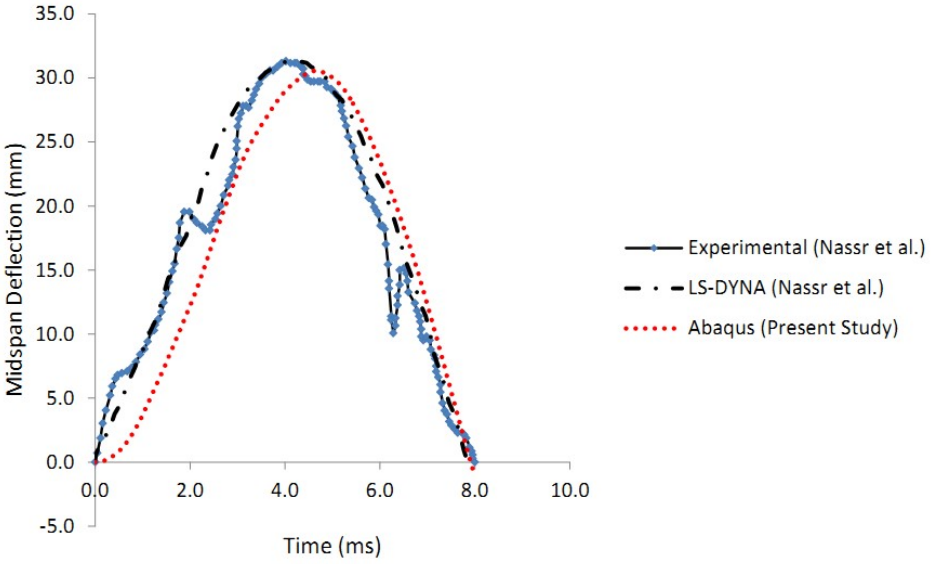

Fig. 12. *Mid-span deflection of C2 column*

4. Optimum Design problem formulation

In general, optimization is a procedure to find the best solution that it satisfies certain conditions. The general form of an optimization problem is as follows:

$$\boldsymbol{min}\, \boldsymbol{F}(\boldsymbol{x}) \tag{10}$$

$$\boldsymbol{Subjected\ to}$$

$$\boldsymbol{g_j(x) = 0\ ; j = 1 \dots \dots m_e}$$

$$\boldsymbol{g_j(x) \geq 0\ ; j = m_e \dots \dots m}$$

Where $F(x)$ is the objective function, $g_j(x)$ are the constraints, x is the design variable vector, m_e is the number of equality constraints, and m is the number of all constraints. Based on the nature of the problem, the optimization procedure can be performed using an appropriate optimization technique. Three numerical optimization techniques are utilized in the current study. These techniques are Nonlinear Programming by Quadratic Lagrangian (NLPQLP), Particle Swarm Optimization (PSO), and Multi Island Genetic Algorithm (MIGA). NLPQLP is a special implementation of Sequential Quadratic Programming (SQP) algorithm. In each iteration of this technique, by a quadratic approximation of Lagrangian function and a linear approximation of constraints, the optimization sub-problems are formulated and solved as a quadratic programming problem. Considering Eq. (10), the Lagrangian function of the problem will be:

$$L(x,u) \coloneqq f(x) - \sum_{j=1}^{m} u_j g_j(x) \tag{11}$$

Where x is the design variable vector and, u is the Lagrange multiplier vector. Quadratic sub-problem in the $k-th$ iteration can be formulated as follow:

$$\min 0.5 d^T C_k d + \nabla f(x_k)^T d \tag{12}$$

$$\nabla g_j(x_k)^T d + g_j(x_k) = 0\ , j = 1, \dots, m_e$$

$$\nabla g_j(x_k)^T d + g_j(x_k) \geq 0\ , j = 1, \dots, m$$

C_k is an approximation of the Hessian of the Lagrangian function, x_k is an approximation of the solution, and the ∇ sign indicates the gradient operator. The solution of this quadratic programming sub-problem is the search direction d. By considering the corresponding Lagrange multiplier of this sub-problem as u_k, and an approximation of the multipliers as v_k, the new iteration is obtained by:

$$\binom{x_{k+1}}{v_{k+1}} \coloneqq \binom{x_k}{v_k} + \alpha_k \binom{d_k}{u_k - v_k} \tag{13}$$

$\alpha_k \in (0,1]$ is a suitable step-length parameter. The step-length parameter is used to have a global convergence, i.e., when starting from an arbitrary design point, the final solution be a point that satisfies the Karush-Kuhn-Tucker optimality conditions. α_k should be taken so that a sufficient decrease in a merit function $\phi_r(\alpha)$ be obtained:

$$\phi_r(\alpha) \coloneqq \psi_r\left(\binom{x_k}{v_k} + \alpha\binom{d}{u-v}\right) \tag{14}$$

$\psi_r\ (x, v)$ is a suitable penalty function. In NLPQLP, this penalty function is the augmented Lagrangian function:

$$\psi_r\ (x, v) \coloneqq f(x) - \sum\left(v_j g_j(x) - 0.5 r_j g_j(x)^2\right) - 0.5 \sum \frac{v_j^2}{r_j} \tag{15}$$

r_j is corresponding penalty parameter that controls the degree of the constraint violation. This parameter must carefully be chosen to guarantee a descent direction of the merit function. The objective function is penalized when a design point leaves the feasible domain. To avoid calculation of the second derivatives, Hessian of the Lagrangian function is started with the identity matrix and is iteratively updated by the BFGS method:

$$C_{k+1} \coloneqq C_k + \frac{q_k q_k^T}{p_k^T q_k} - \frac{C_k p_k p_k^T C_k}{p_k^T C_k p_k} \tag{16}$$

Where,

$$q_k \coloneqq \nabla_x L(x_{k+1}, u_k) - \nabla_x L(x_k, u_k)\ and\ p_k \coloneqq x_{k+1} - x_k \tag{17}$$

The main convergence criteria in NLPQLP are based on numerically satisfying the KKT (Karush-Kuhn-Tucker) optimality conditions. When the KKT conditions are satisfied with a desired tolerance, the algorithm will stop. More details about this technique are available in NLPQLP User Guide (Schittkowski, 2006). It should be noted that in such engineering problems the structural responses (functions) are not explicitly available. Thus, for obtaining derivatives required in the optimization algorithm, sensitivity analysis can be performed. This can be done easily using finite different procedure, as forward or central difference methods. The derivative of a structural response f according to the design variable x can be approximated using forward difference formula as follows:

$$\frac{df}{dx} = \frac{f(x+h) - f(x)}{h} \tag{18}$$

Also, the central difference formula can be written as follows:

$$\frac{df}{dx} = \frac{f(x+h) - f(x-h)}{2h} \tag{19}$$

If there are n number of design variables, to obtain the sensitivity of structural responses with respect to all design variables, n structural analysis are required using the forward difference formula and $2n$ structural analysis are required using the central difference formula. Thus, the computational effort in the central difference method is higher than the forward difference, but it is more accurate. In the NLPQLP optimizer the main configuration parameter is the finite difference step size. The step size should be chosen small enough to reduce the error of evaluating gradients. In some structural problems which the structural analysis is poor, choosing very small step sizes may lead to unstable optimization process.

The Particle Swarm Optimization (PSO) algorithm was firstly developed by Kennedy and Eberhart (1995). This algorithm is a population based optimization technique, which is inspired by social behavior of bird flocking or fish schooling. This algorithm has many similarities with evolutionary algorithms such as Genetic Algorithms (GA). But unlike the GA, no evolution operators such as crossover and mutation are used in PSO. In this algorithm, the potential solutions, called particles, fly through the problem space by following the current optimum particles. The best position found by a particle and its neighbors is used to decide the next position of the particle in the next iteration. The condition of a particle is the value for all design variables in the optimization problem and its velocity in the design space, and each move produces a new generation. The particle swarm algorithm starts by generating a set of random particles that make the initial population as the initial design. Also initial velocities are given to the particles. In each iteration of the algorithm, the particle is moved using two best values. The first one

is the best position found by the particle (particle-best or $\bar{P}_{best}$) and the second one is the best value obtained by all particles among all the generations so far (global-best or $\bar{G}_{best}$).

We assume that $\bar{X}_i^j$ and $\bar{V}_i^j$, are the current position and velocity of the particle i during iteration j, respectively. The velocity and position of the particle in the next iteration, (j+1), is obtained as follows:

$$\bar{V}_i^{j+1} = I\bar{V}_i^j + r_1 P_{Incr}\left(\bar{P}_{best} - \bar{X}_i^j\right) + r_2 G_{Incr}\left(\bar{G}_{best} - \bar{X}_i^j\right) \tag{20}$$

$$\bar{X}_i^{j+1} = \bar{X}_i^j + \bar{V}_i^{j+1} \tag{21}$$

r_1 and r_2 are random numbers which are between 0 and 1, I is the particle's inertia. The Inertia can be set to any positive value. But in many researches the value for Inertia is chosen around 1. For example Shi and Eberhart (1998) concluded that the Inertia between 0.9 and 1.2 works well. By selecting a larger value for the inertia the particle can explore a larger domain of the design space, but this increases the number of iterations needed to converge to the optimum design. P_{Incr} and G_{Incr} are called "Learning Factors" which are the maximum increments due to particle-best and the maximum increments due to global-best, respectively. Generally the value of P_{Incr} and G_{Incr} are set to 0.9. More details about the PSO optimization algorithm can be reviewed in (Kennedy, 2011).

Multi Island Genetic Algorithm (MIGA) (Miki et al, 1999) is an improved version of genetic algorithm (GA). The main difference of MIGA from the traditional GA is that in (MIGA) each population of individuals is divided into several sub-populations called "islands." All of the traditional GA operations including selection, crossover, and mutation are performed on each sub-population. Some individuals are selected from each island and migrated to different islands periodically during an operation called "migration". The migration is controlled by two parameters which are "migration interval" and "migration rate". Migration interval is the number of generations between each migration, and migration rate is the percentage of individuals migrated from each island. More details about MIGA algorithm can be reviewed in (Miki et al., 1999).

The purpose of a structural optimization is to find the design variables for a structural system in order to maximize or minimize the objective function, and to satisfy the design requirements. Since there is a direct correlation between the weight of a structure and the cost of materials and construction, in many structural optimization problems the structural weight is considered as the objective function which must be minimized to achieve the lowest cost. In the current study the structural weight is considered as the objective function which is being minimized during the optimization process. Also in structural problems, depending on the problem, various constraints such as stress, frequency, and deformation may be considered. As blast loads usually are such that the structural responses may go in inelastic zone, appropriate consideration of nonlinear analysis should be taken into account. In an inelastic design it is better not to consider the strength constraints (Gong et al. 2012). Zieman et al. (1992) showed that an inelastic design could not be used to full advantage if a design is required to satisfy both strength and deformation constraints, as the strength constraints generally prevent the structural member from yielding. Accordingly, in the present study, only the deformation constraints are taken into account. According to the UFC 3-340-02 (2008) criteria, design constraints are considered as story drifts and relative support rotation in beams and columns. Based on these criteria, maximum allowable story drift is $H_s/25$ which H_s is the height of the $s-th$ story, and the maximum allowable relative support rotation in beams and columns for frame members is limited to 2 degrees (0.035 rad). It should be noted that based on the UFC code, the relative support rotation in members are measured as the angle between the maximum deflection point and the member's chord, as shown in Figs 13 and 14.

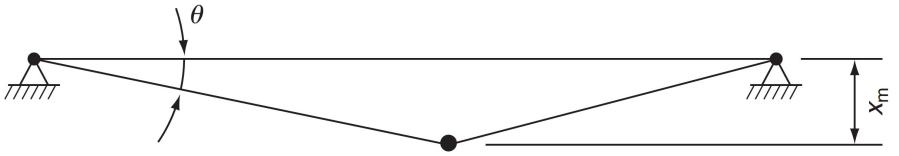

Fig. 13. *Relative support rotation in beam members (UFC 3-340-02, 2008)*

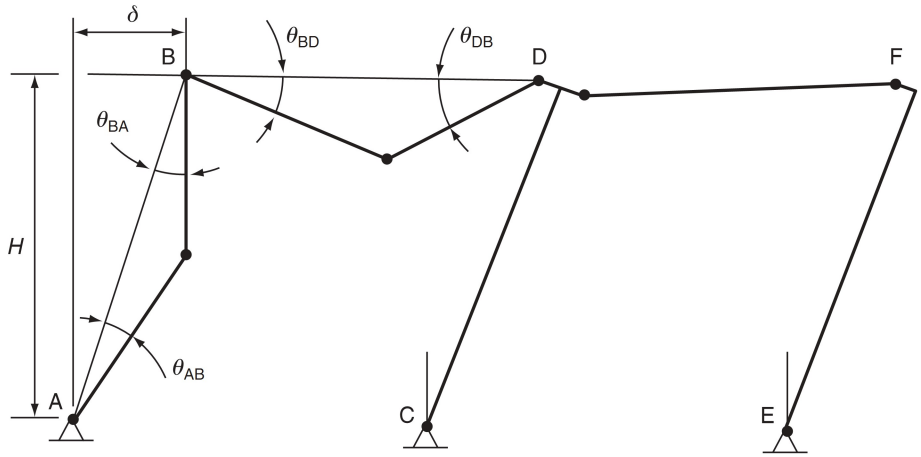

Fig. 14*. Relative support rotation in frame members (UFC 3-340-02, 2008)*

Based on the above considerations the design problem formulation is considered as follows:

$$\boldsymbol{Min}\ \sum(\boldsymbol{\gamma L_m A_m})\ (\boldsymbol{m = 1, \dots\dots\dots, n_m}) \tag{22}$$

$\boldsymbol{Subject\ to}$:

$$\boldsymbol{\varphi_{m,max} \leq \varphi_{all}}$$

$$\boldsymbol{\delta_{s,max} \leq \delta_{s,all}\ (S = 1, \dots\dots\dots, n_s)}$$

Where γ is the material specific weight that equals to 7850 (kgf/m^3), L_m is the length of the $m-th$ member, A_m is the cross-sectional area of the $m-th$ member, n_m is the number of members, $\varphi_{m,max}$ is the maximum support rotation of $m-th$ member, φ_{all} is the allowable support rotation of members, $\delta_{s,max}$ is the maximum story drift of $s-th$ story, $\delta_{s,all}$ is the allowable drift for $s-th$ story, and n_s is the number of stories. It should be noted that the drift of a story is measured as the difference between the lateral displacements of that story and its lower story.

Here, based on the discussed assumptions an optimization methodology is proposed and assessed for optimum design of steel frames against blast loading. The flowchart of the proposed method is shown in Fig 15. As described in Fig 15, after numerical modeling of the structure, the model is initialized. This includes applying gravitational and blast loads on the structure and initializing the design variables. In the present research, the cross-sectional areas of members are considered as the design variables. The other geometrical properties of the sections such as section depth, width, flange and web thicknesses are computed based on some equations of cross-sectional areas. These equations can be easily derived by performing regression analysis on available steel profile sections such as American AISC or European DIN 1025 I-shape sections, or other available sections. In the next step the structural analysis is performed to derive the structural responses. In the present study, the structural analysis is carried out by explicit nonlinear dynamic finite element analysis of the structure, using Abaqus FE analysis software. As previously mentioned, using explicit nonlinear dynamic FE analysis in blast analysis problems, in addition of its high accuracy, also is relatively computationally inexpensive. After deriving the nonlinear responses the optimization problem can be formulated based on UFC-3-340-02 criteria. In the next step, by using numerical optimization techniques and based on the design formulation, an optimization step will be performed. In the case of using gradient based optimization techniques, the sensitivity analysis is required to be able to use the technique. As the structural analysis is performed using nonlinear FE analysis, the structural sensitivities can be calculated with a suitable accuracy. More accurate sensitivities result in more accurate and stable optimization procedure in the case of gradient based techniques. The design procedure is repeated until stopping criteria are satisfied. At the end, cross sectional areas and the weight of the structure at the optimum point are reported as the optimum results. According to the proposed methodology a framework is developed and some numerical examples are studied. In the next section three numerical examples are presented by assessing three numerical optimization techniques of NLPQLP, PSO, and MIGA, using the proposed method and the developed framework.

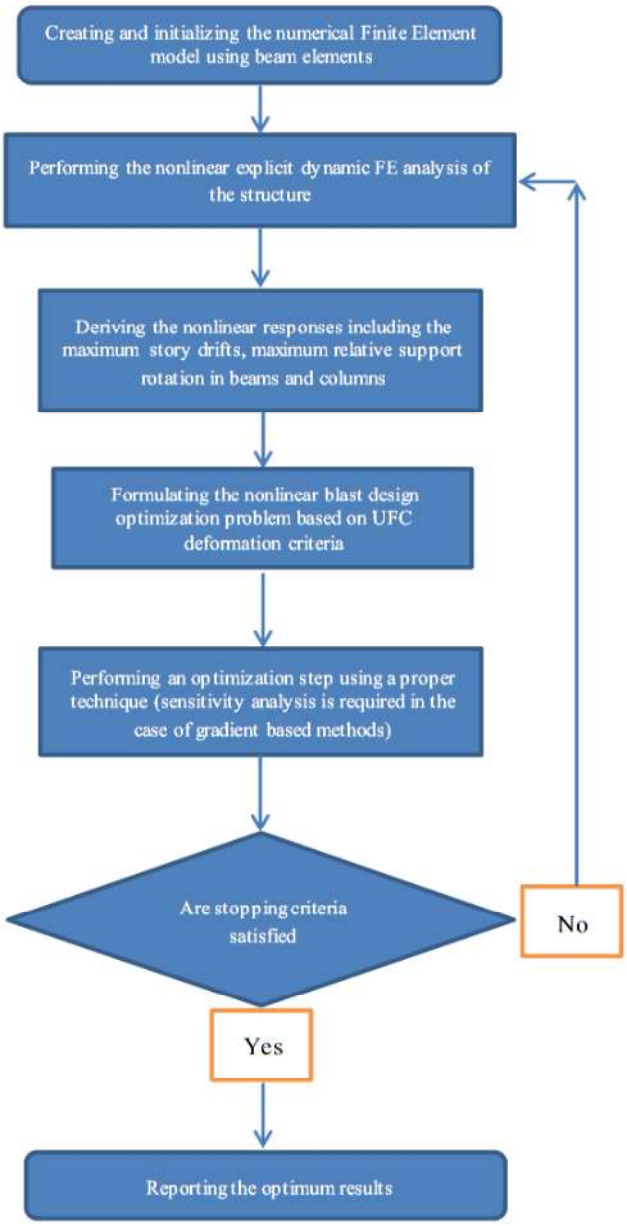

Fig. 15. Flowchart of the proposed method

5. Numerical Examples

The following assumptions are made throughout the studied examples:

Three types of loading are considered which are dead, live and blast loads. In all stories dead and live loads are assumed to be $6kN/m^2$ and $2kN/m^2$, respectively. The tributary widths of the studied frames are assumed to be 4 m. It is assumed that based on the blast threat analysis, the structures are designed for a surface blast of 150 kg TNT equivalent and a standoff distance of 15 m. As the scaled blast distance is $2.82 > 1.2\ m/kg^{1/3}$, the explosion is classified as far-range blast. Thus, the blast loading profile has been assumed as a uniform time-history loading acting on the front side of the structure. Also, as proposed in Handbook for Blast-Resistant Design of Buildings (Dusenberry, 2010), the load combination is considered as:

1.0 DL+0.25 LL+1.0 B

Where DL is the dead load, LL is the live load, and B is the blast load acting on the structure.

Design constraints are considered based on UFC 3-340-02 (2008) criteria. These constraints are the maximum story drift and relative support rotation in beams and columns. Based on the UFC criteria, allowable drift is limited to H/25, and the allowable relative support rotation is limited to 2 degrees (0.035 rad). The weight

of the structure is considered as the objective function which is minimized during the optimization process. For all members Yield stress is $240Mpa$, and Ultimate stress is $360Mpa$. Since the assumed yield stress of steel is 240 MPa, and this value is very close to the yield stress of ASTM A36 (Fy=250 MPa), thus, the DIF data of ASTM A36 (the red curve in Fig 5) are used in FE modeling of the numerical examples. Design variables are the cross-sectional areas of members. Other geometrical properties of frame member sections have been formulated based on the European DIN 1025 standard profiles, as $6th$ order polynomial functions of the cross-sectional areas. IPB (HEB) profiles are used for columns, and IPE profiles are used for beam members. Design variables are assumed as continuous variables in the design space. Lower bound limit of the columns cross-sectional areas is set to 4300 mm^2 corresponding to IPB 14 and the upper bound is limited to 19800 mm^2 corresponding to IPB 40. Similarly, the Lower bound of the beams cross-sectional areas is limited to 2010 mm^2 corresponding to IPE 16 and the upper bound is limited to 8450 mm^2 corresponding to IPE 40. It should be noted that the configuration parameters for all of the optimization methods are considered to be in a conventional and standard range. All the considered examples are solved by parallel processing using a laptop computer with Intel Core i5 processor and 4 GB RAM.

5-1. One-story one-bay portal frame

In this example, the optimum design of a one-story portal frame is performed. The frame topology is shown in Fig 16. Two groups of sections are considered in the design: one group for columns and another one for beam. These section groups are shown in Fig. 16 using numbers 1 and 2. The frame is optimized using the developed framework by three techniques of NLPQLP, PSO, and MIGA. The initial configuration of the optimization techniques are summarized in Tables 3-5. Table 6 shows the initial values of the variables and the objective function. Table 7 shows a comparison between the results of the three techniques at the optimum point. Also Convergence history is shown in Fig. 17 for 100 design evaluations. It can be seen that the optimum design obtained by NLPQLP has a weight 26% lighter than the initial design. Also optimum weight obtained by NLPQLP is 3.8% lighter than PSO and 6.12% lighter than MIGA optimum solutions. Total execution time for performing the optimization process using NLPQLP technique is 79% lower than the execution time required for PSO and 77% lower than the execution time required for MIGA. It is obvious that in this example, NLPQLP technique has a faster convergence and needs less computational efforts comparing to MIGA and PSO techniques.

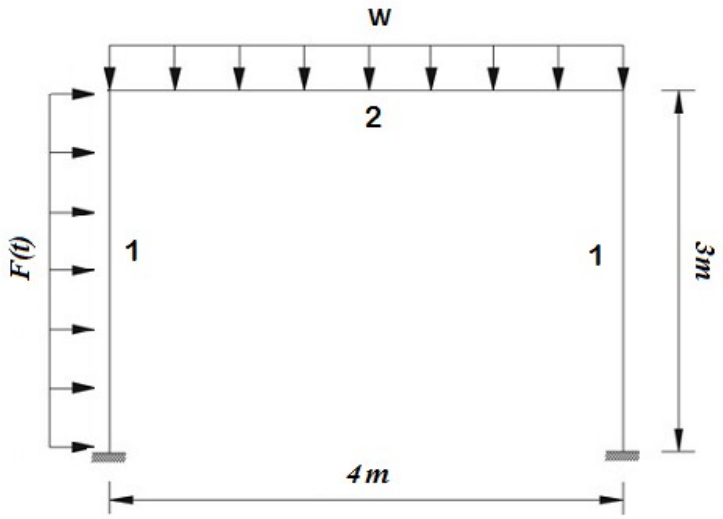

Fig. 16. *Frame dimensions, gravitational and blast loading for one story example*

Table 3. *Initial configuration of the NLPQLP optimizer in the first example*

Technique	NLPQLP (SQP)
Finite Difference method	Forward difference
Relative finite difference step size	0.002
Minimum finite difference step size	1e-6

Table 4. *Initial configuration of the PSO optimizer in the first example*

Technique	Particle Swarm Optimization (PSO)
Maximum iterations	20
Number of particles	5
Inertia	0.9
Global increment	0.9
Particle increment	0.9
Maximum velocity limit	0.1

Table 5. *Initial configuration of the MIGA optimizer in the first example*

Technique	MIGA
Subpopulation size	5
Number of islands	2
Number of generations	10
Crossover rate	1
Mutation rate	0.01
Migration rate	0.01
Migration interval	5

Table 6. *Starting point properties for the one-story example*

	NLPQLP	PSO	MIGA
$A_1\ (mm^2)$	19800	random	random
$A_2\ (mm^2)$	8450	random	random
$Weight\ (kN)$	11.98	-----	-----

Table 7. *Optimum point properties for the one-story example*

	NLPQLP	PSO	MIGA
$A_1\ (mm^2)$	13460	15897	16905
$A_2\ (mm^2)$	8122	5582	4793
$Weight\ (kN)$	8.89	9.24	9.47
$Number\ of Runs$	16	100	100
$time$	3':52"	18':28"	16':45"

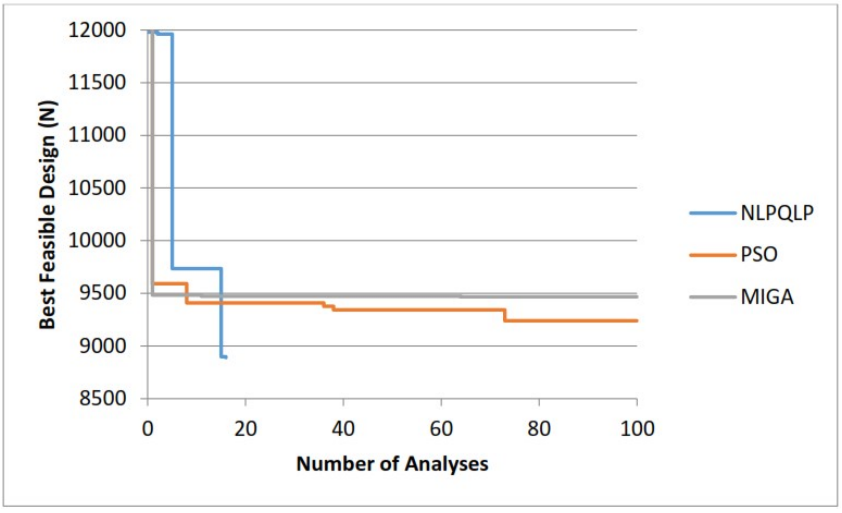

Fig. 17. *convergence history of the one-story example*

5-2. Three-story two-bay frame

The second example is a three-story two-bay frame shown in Fig. 18. Design section groups are categorized into six groups as shown in Fig. 18 by numbers 1 to 6. The optimization procedure is performed using the developed framework by three optimization techniques of NLPQLP, PSO, and MIGA. The initial configuration of the optimization techniques are summarized in Tables 8-10. Table 11 shows the initial values of the variables and the objective function. Table 12 shows a comparison between the results of the three techniques at the optimum point. Convergence history is shown in Fig.19 for 250 design evaluations. It is evident that the optimum design obtained by NLPQLP has a weight 14% lighter than the initial design. Also optimum weight obtained by NLPQLP is 2.3% lighter than PSO. In this example no feasible design found using MIGA technique through the 250 runs. Total execution time for performing the optimization process using NLPQLP technique is 62% lower than the execution time required for PSO and 61% lower than the execution time required for MIGA. Like the previous example, NLPQLP technique shows faster convergence and better results comparing to the MIGA and PSO techniques.

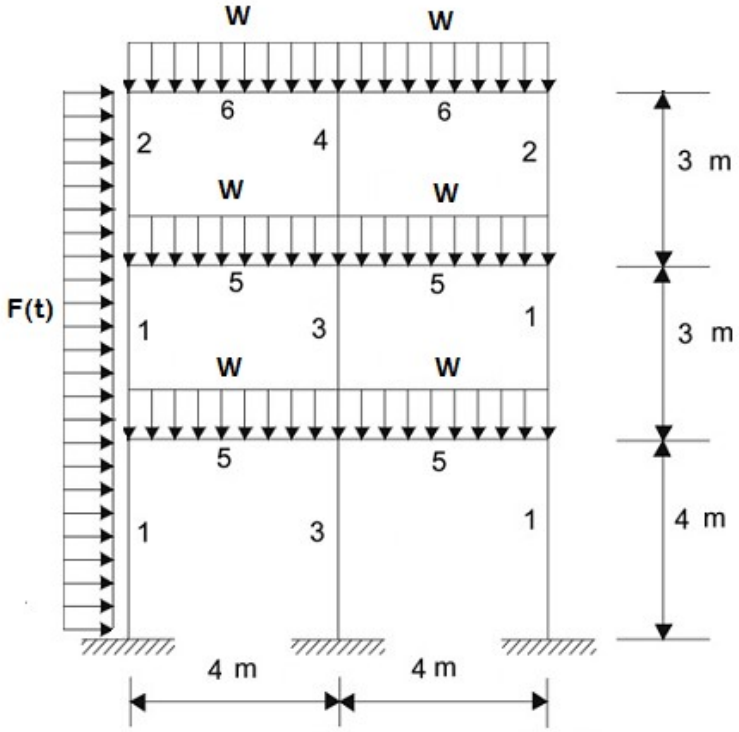

Fig. 18. *Frame dimensions, gravitational and blast loading for the three story example*

Table 8. *Initial configuration of the NLPQLP optimizer in the second example*

Technique	NLPQLP (SQP)
Finite Difference method	Forward difference
Relative finite difference step size	0.003
Minimum finite difference step size	1e-8

Table 9. *Initial configuration of the PSO optimizer in the second example*

Technique	Particle Swarm Optimization (PSO)
Maximum iterations	25
Number of particles	10
Inertia	0.9
Global increment	0.9
Particle increment	0.9
Maximum velocity limit	0.1

Table 10. *Initial configuration of the MIGA optimizer in the second example*

Technique	MIGA
Subpopulation size	5
Number of islands	5
Number of generations	10
Crossover rate	1
Mutation rate	0.01
Migration rate	0.01
Migration interval	5

Table 11. *Starting point properties for the three story example*

	NLPQLP	PSO	MIGA
$A_1(mm^2)$	19800	Random	Random
$A_2(mm^2)$	19800	Random	Random
$A_3(mm^2)$	19800	Random	Random
$A_4(mm^2)$	19800	Random	Random
$A_5(mm^2)$	8450	Random	Random
$A_6(mm^2)$	8450	Random	Random
$Weight\ (kN)$	62.55	-----	-----

Table 12. *Optimum point properties for the three story example*

	NLPQLP	PSO	MIGA
$A_1(mm^2)$	19800	19800	---
$A_2(mm^2)$	13332	16126	---
$A_3(mm^2)$	19123	19800	---
$A_4(mm^2)$	9822	4300	---
$A_5(mm^2)$	8438	8450	---
$A_6(mm^2)$	3802	5211	---
$Weight\ (kN)$	53.85	55.13	---
$Number\ of\ Runs$	52	250	250
$time$	20':10"	52':51"	51':42"

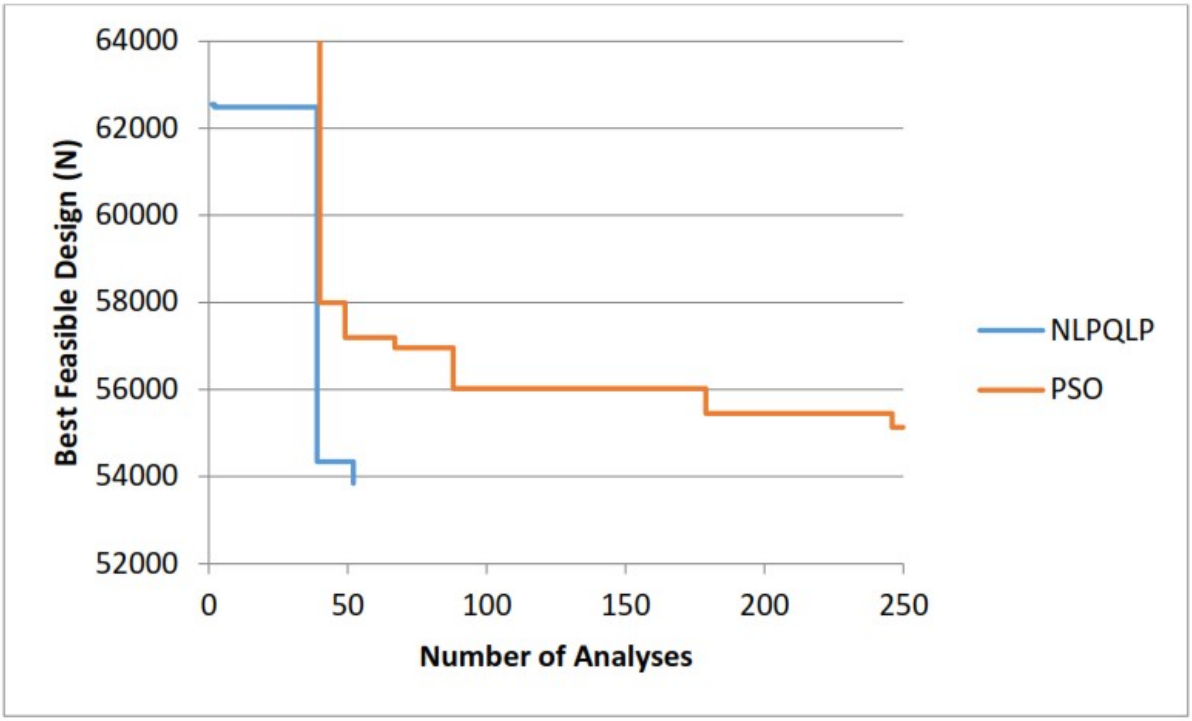

Fig 19. *convergence history of the second example*

5-3. Six-story three-bay frame

The third example is a six-story three-bay frame shown in Fig 20. Design sections are categorized into nine groups as shown in Fig. 20 by numbers 1 to 9. Using the developed framework this frame is optimized by three optimization algorithms of NLPQLP, PSO, and MIGA. The initial configuration of the optimization techniques are summarized in Tables 13-15. Table 16 shows the initial values of the design variables and the structural weight. Table 17 shows a comparison between the results of the three techniques at the optimum point. Convergence history is shown in Fig.21 for 500 design evaluations. It is evident that the optimum design obtained by NLPQLP has a weight 30% lighter than the initial design. Also optimum weight obtained by NLPQLP is 8.5% lighter than PSO. For MIGA method, no feasible design was found through the 500 runs. Also, total execution time for performing the optimization process using NLPQLP technique is 67% lower than the execution time required PSO and 65% lower than the execution time required for MIGA. Just like the previous examples, the NLPQLP technique has a faster convergence and better results comparing to MIGA and PSO techniques.

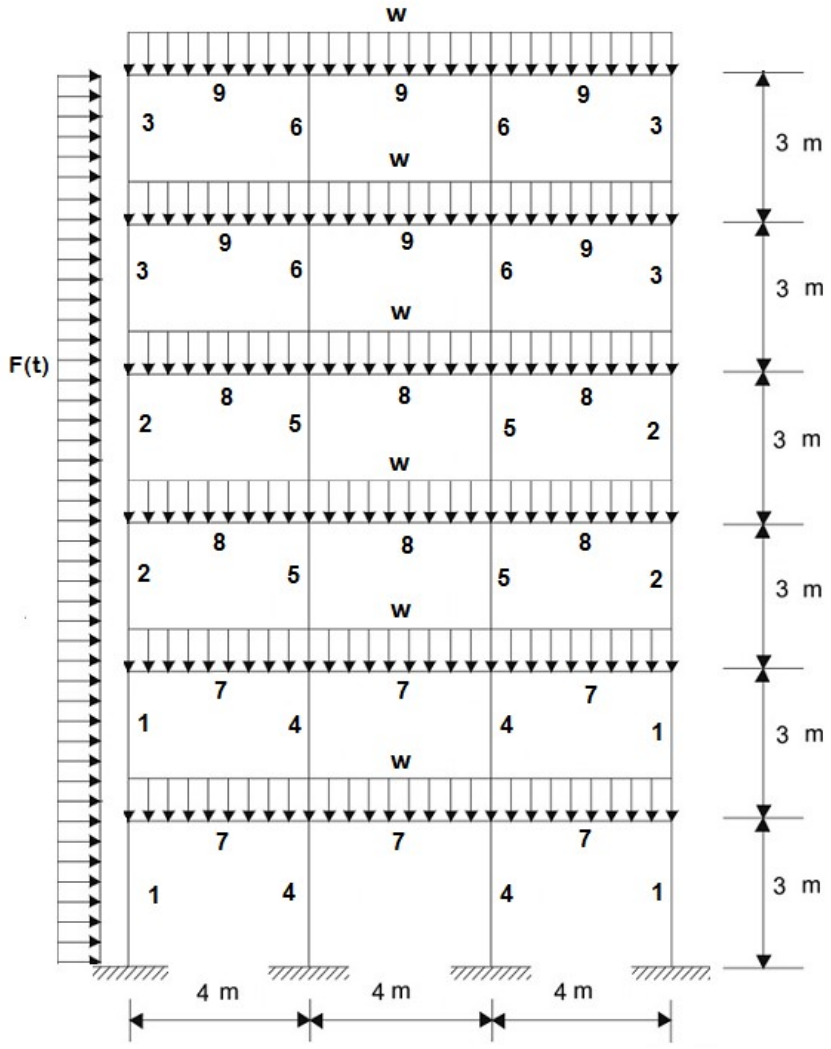

Fig. 20. *Frame dimensions, gravitational and blast loading for the five story example*

Table 13. *Initial configuration of the NLPQLP optimizer in the third example*

Technique	NLPQLP (SQP)
Finite Difference method	Forward difference
Relative finite difference step size	0.01
Minimum finite difference step size	1e-8

Table 14. *Initial configuration of the PSO optimizer in the third example*

Technique	Particle Swarm Optimization (PSO)
Maximum iterations	50
Number of particles	10
Inertia	0.9
Global increment	0.9
Particle increment	0.9
Maximum velocity limit	0.1

Table 15. *Initial configuration of the MIGA optimizer in the third example*

Technique	MIGA
Subpopulation size	10
Number of islands	5
Number of generations	10
Crossover rate	1
Mutation rate	0.01
Migration rate	0.01
Migration interval	5

Table 16. *starting point properties in the third example*

	NLPQLP	PSO	MIGA
$A_1(mm^2)$	19800	Random	Random
$A_2(mm^2)$	19800	Random	Random
$A_3(mm^2)$	19800	Random	Random
$A_4(mm^2)$	19800	Random	Random
$A_5(mm^2)$	19800	Random	Random
$A_6(mm^2)$	19800	Random	Random
$A_7(mm^2)$	8450	Random	Random
$A_8(mm^2)$	8450	Random	Random
$A_9(mm^2)$	8450	Random	Random
$Weight\ (kN)$	159.67	-----	-----

Table 17. *optimum point properties for the third example*

	NLPQLP	PSO	MIGA
$A_1(mm^2)$	14340	14622	---
$A_2(mm^2)$	13476	19587	---
$A_3(mm^2)$	16852	15851	---
$A_4(mm^2)$	13078	16371	---
$A_5(mm^2)$	11209	13191	---
$A_6(mm^2)$	5694	4300	---
$A_7(mm^2)$	8450	7349	---
$A_8(mm^2)$	7852	7001	---
$A_9(mm^2)$	5612	8450	---
$Weight\ (kN)$	111.61	122	---
Number of Runs	145	500	500
Total time	50':16"	2:30':49"	2:23':47"

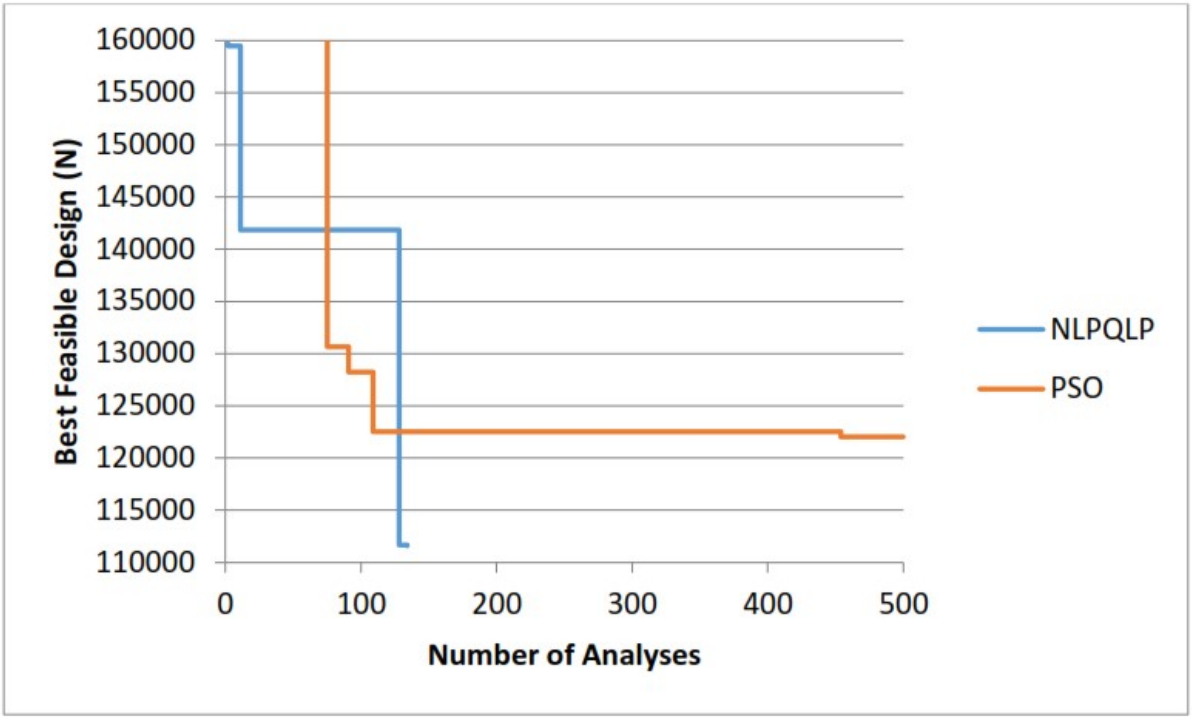

Fig 21. *convergence history of the third example*

6. Conclusions

In this study, optimum design of steel moment frames under blast loading was studied. For this purpose, first an optimization algorithm was proposed. The structural analysis in the proposed method is performed using nonlinear explicit dynamic finite element analysis. The nonlinear dynamic finite element analysis results in relatively accurate and realistic evaluations of structural responses. Unlike the seismic analysis problems, In the case of blast loading, the explicit dynamic analysis is very computationally effective. Based on the proposed method a framework was developed and three numerical optimization techniques were investigated through the numerical examples. Results of the numerical examples show that the NLPQLP technique was superior to the other studied optimization techniques, in the current blast optimum design problem. The NLPQLP technique had better results than the two other optimization techniques and found better designs in lower number of runs. Also, between the two methods of PSO and MIGA, the PSO method had better results. Also, the computational time of the PSO and the MIGA methods were approximately the same. Results of this research show that by using the nonlinear explicit FE analysis as the structural analysis method and NLPQLP method as the optimization technique, the optimum design of steel frames under blast loading, can be performed very effectively, because the procedure is relatively precise and computationally cost effective. Also, since the NLPQLP resulted in better optimum points comparing to the PSO and MIGA methods, the NLPQLP method is capable of converging to the global optima in the current problem. In the future researches, the effectiveness of other numerical optimization techniques can be studied for the problem of optimization of steel frames under blast loading.

References

Artar, M. (2016). “Optimum design of braced steel frames via teaching learning based optimization”. STEEL AND COMPOSITE STRUCTURES, 22(4), 733-744.

ASCE 59-11 (2011), “Blast Protection of Buildings”, American Society of Civil Engineers, Reston, VA, USA.

Coffield, A., Adeli, H. (2014), “An investigation of the effectiveness of the framing systems in steel structures subjected to blast loading”, Journal of Civil Engineering and Management, 20(6), 767-777.

Cormie, D., Mays, G., Smith, P. (2009), "Blast Effects on Buildings (Second Edition)", Thomas Telford Publishing, London, UK.

De Borst, R., Crisfield, M. A., Remmers, J. J., Verhoosel, C. V. (2012) "Nonlinear Finite Element Analysis of Solids and Structures (Second Edition)", John Wiley & Sons.

Degertekin, S. O. (2012). "Optimum design of geometrically non-linear steel frames using artificial bee colony algorithm". Steel and Composite Structures, 12(6), 505-522.

Dusenberry, D.O. (2010). "Handbook for Blast-Resistant Design of Buildings", Jon Wiley & Sons, Hoboken, NJ.

Elsanadedy, H.M., Almusallam, T.H., Alharbi, Y.R., Al-Salloum, Y.A., Abbas, H. (2014), "Progressive collapse potential of a typical steel building due to blast attacks", Journal of Constructional Steel Research, 101, 143-157.

FEMA 452 (2005), "A How to Guide to Mitigate Potential Terrorist Attacks Against Buildings", Federal Management Agency, Washington (DC), USA.

Gholizadeh, S., Davoudi, H., Fattahi, F. (2017) "Design of steel frames by an enhanced moth flame optimization algorithm", Steel and Composite Structures, 24(1), 129-140.

Gong, Y., Xue, Y., Xu, L., Grierson, D.E. (2012), "Energy-Based design optimization of steel building frameworks using nonlinear response history analysis", Journal of Constructional Steel Research, 68, 43-50.

Hibbitt, H., Karlsson, B., & Sorensen, P. (2010). "Abaqus analysis user's manual version 6.10". Dassault Systèmes Simulia Corp.: Providence, RI, USA.

Habibi, A.R, Rostami, H. (2013), "Optimum design of plane Steel moment frames by using consistent approximation method", MSc. Thesis, University of Kurdistan, Sanandaj, Iran.

Habibi, A.R., Khaledy, N. (2015), "Development of an Exact Method to Analyze Beam-Columns Subjected to Blast", Journal of passive deffence, 5(4), 21-28.

Hadianfard, M. A., Farahani, A., Jahromi, A. (2012). "On the effect of steel columns cross sectional properties on the behaviours when subjected to blast loading". Structural Engineering and Mechanics, 44(4), 449-463.

Kaveh, A., Fahimi-Farzam, M., & Kalateh-Ahani, M. (2015). "Optimum design of steel frame structures considering construction cost and seismic damage". Smart Structures and Systems, 16(1), 1-26.

Kaveh, A., Farahmand Azar, B., Hadidi, A., Rezazadeh Sorochi, F., Talatahari, S. (2010), "Performance based Seismic design of steel frames using ant colony optimization", Journal of Constructional Steel Reseach, 66, 566-574.

Kaveh, A., Nasrollahi, A. (2014), "Performance-based seismic design of steel frames utilizing charged system search optimization", Applied Soft Computing, 22, 213-221.

Kennedy, J. (2011). "Particle swarm optimization". Encyclopedia of machine learning (pp. 760-766). Springer US.

Kennedy, J, and R Eberhart. (1995). "Particle Swarm Optimization." In Proceedings of ICNN'95 - International Conference on Neural Networks, 4:1942–48. IEEE.

Miki, M., Hiroyasu, T., Kaneko, M., & Hatanaka, K. (1999). "A parallel genetic algorithm with distributed environment scheme". Systems, Man, and Cybernetics, 1999. IEEE SMC'99 Conference Proceedings. 1999 IEEE International Conference on (Vol. 1, pp. 695-700). IEEE.

Nassr, A.A., Razaqpur, A.Gh., Tait, M.J., Campidelli, M., Foo, S. (2012), "Single and multi-degree of freedom analysis of steel beams under blast loading", Nuclear Engineering and Design, 242, 63-77.

Nassr, A.A., Razaqpur, A.Gh., Tait, M.J., Campidelli, M., Foo, S. (2013), "Strength and and stability of steel beam columns under blast load", International Journal of Impact Engineering, 55, 34-48.

Nassr, A.A. (2012), "Experimental and Analytical Study of the Dynamic Response of Steel Beams and Columns to Blast Loading", PhD Thesis, McMaster University, Canada.

Qi, Ch., Yang, Sh., Yang, L.J., Wei, Zh.Y., Lu, Zh. H. (2013), "Blast resistance and multi-objective optimization of aluminum foam-cored sandwich panels, Composite Structures, 105, 44-57.

Saeed Monir, H. (2013), "Flexible blast resisitant steel structures by using unidirectional passive dampers", Journal of Constructional Steel Research, 90, 98-107.

Salimi, H., Saranjam, B., Hoseini Fard, A., Ahmadzadeh, M. (2012), "Use of Genetic Algorithms for Optimal Design of Sandwich Panels Subjected to Underwater Shock Loading", Journal of Mechanical Engineering, 58 (3), 156-164.

Schittkowski, K. (2006). "NLPQLP: A Fortran implementation of a sequential quadratic programming algorithm with distributed and non-monotone line search-user's guide".

Shi, Y., Eberhart, R. (1998). "A modified particle swarm optimizer. Evolutionary Computation Proceedings". IEEE World Congress on Computational Intelligence. The 1998 IEEE International Conference, 69-73.

Sun, W. (2011), "Dynamic Response Analysis and Optimal Design of a RC Slab to Blast Loads", Advanced Materials research, 163-167, 2390-2396.

Taha, M.R, Colak-Altunc, A.B., Al-Halik, M. (2009), "A multi-objective optimization approach for design of blast-resistant composite laminates using carbon nanotubes", Composites: Part B, 40, 522-599.

Taylor, G.I. (1940), "Notes on the Dynamics of Shock Waves from Bar Explosive Charges", UK Ministry of Home Security, Civil Defense Research Committee Paper.

Taylor, G.I. (1941a), "The Propagation and Decay of Blast Waves", UK Home Office, ARP department.

Taylor, G.I. (1941b), "The Propagation of Blast Waves over the Ground", UK Ministry of Home Security, Civil Defence Research Committee paper.

UFC 3-340-02 (2008), "Structures to resist the effects of accidental explosions", US Department of Defense, Washington (DC), USA

Xia, Y., Wu, Ch., Li, Zh. X. (2015), "Optimized Design of Foam Cladding for Protection of Reinforced Concrete Members under Blast Loading", ASCE Journal of Structural Engineering, ASCE J. Struct. Eng, 141(9), 1-7.

Zieman, R.D., Mc Guire, W., Deierlein, G. (1992), "Inelastic limit states design, part I: planar frame studies", ASCE Journal of Structural Engineering, 118 (9), 2532-2549.